Catal Lett (2009) 127:55–62
DOI 10.1007/s10562-008-9759-z

Effect of Ceria on the Sulfation and Desulfation Characteristics of a Model Lean NO_x Trap Catalyst

Yaying Ji · Todd J. Toops · Mark Crocker

Received: 11 September 2008 / Accepted: 29 October 2008 / Published online: 18 November 2008
© Springer Science+Business Media, LLC 2008

Abstract The effect of ceria addition on the sulfation and desulfation characteristics of a model Ba-based lean NO_x trap (LNT) catalyst was studied. According to DRIFTS and NO_x storage capacity measurements, ceria is able to store sulfur during catalyst exposure to SO_2, thereby helping to limit sulfation of the main (Ba) NO_x storage phase and maintain NO_x storage capacity. Temperature programmed desulfation experiments revealed that desulfation of a model ceria-containing catalyst occurred in two stages, corresponding to sulfur elimination from the ceria phase at ~450 °C, followed by sulfur loss from the Ba phase at ~650 °C. Significantly, the ceria-containing catalyst displayed relatively lower sulfur evolution from the Ba phase than its non-ceria analog, confirming that the presence of ceria lessened the degree of sulfur accumulation on the Ba phase.

Keywords Lean NO_x trap · NO_x adsorber · Sulfation · Desulfation · Ceria

1 Introduction

Lean NO_x Trap (LNT) catalysts, also known as NO_x Storage-Reduction (NSR) catalysts, represent a promising technology for the abatement of NO_x from lean burn internal combustion engines. LNT catalysts typically contain precious metals (generally Pt and Rh) and an alkali or alkaline earth metal storage component (most commonly BaO) supported on a high surface area metal oxide. Under lean exhaust conditions, NO is oxidized to NO_2 over the precious metal sites in the catalyst and reversibly stored as nitrates or nitrites on the storage material. Stored NO_x species are subsequently released and reduced to N_2 during short periodic excursions to rich (i.e., net reducing) conditions. The trapping ability of the LNT catalyst is thus restored after a lean-rich cycle [1].

Although LNT catalysts have been commercialized for lean-burn gasoline and diesel applications in Europe, Japan and North America, the issue of catalyst durability remains problematic. LNT susceptibility to sulfur poisoning is the single most important factor determining effective catalyst lifetime. The NO_x storage element of the catalyst has a greater affinity for SO_x than it does for NO_x, and the resulting sulfate is more stable than the stored nitrate. Although this sulfate can be removed from the catalyst by means of high temperature treatment under rich conditions, the required conditions give rise to deactivation mechanisms such as precious metal sintering, loss of washcoat surface area, and solid state reactions between the various oxides present [1, 2].

In an effort to enhance the sulfur resistance of LNT catalysts, various catalyst modifications have been proposed. Yamazaki et al. [3] incorporated Fe into Ba-based LNT catalysts and found that its addition decreased sulfur uptake and promoted the decomposition of $BaSO_4$. Fanson et al. [4] observed an increase in the durability of LNT catalysts when incorporating Fe into Ba-based LNT catalysts, this being attributed to the ability of Fe to support the formation of a bulk nitrate species that is resistant to the effects of SO_2. Other researchers have reported that the

Y. Ji · M. Crocker (✉)
Center for Applied Energy Research, University of Kentucky,
2540 Research Park Drive, Lexington, KY 40511, USA
e-mail: crocker@caer.uky.edu

T. J. Toops
Oak Ridge National Laboratory, Fuels, Engines and Emissions
Research Center, 2360 Cherahala Blvd., Knoxville, TN 37932,
USA

addition of Mg can mitigate sulfur deactivation of the Ba phase in LNT catalysts [5]. Storage materials other than BaO/Al_2O_3 have also been studied and in some cases have been reported to show enhanced sulfur tolerance. Examples include TiO_2 [6], $BaSnO_3$ [7], and Li_2O supported on metal oxides such as Al_2O_3 [8] and TiO_2 [9]. The use of Cu-containing catalysts has also been examined [10, 11], the Cu being added in addition to or in place of Pt. In these cases, the improvement in catalyst sulfur tolerance was ascribed at least in part to the inability of Cu to oxidize SO_2.

Another approach focuses on the use of support materials with improved sulfur tolerance. Matsumoto and co-workers [12, 13] concluded that increasing the acidity of the alumina used for supporting the Ba phase, by doping with an acidic oxide such as titania, lessened the degree of sulfur adsorption. Furthermore, they found that a Ba-based LNT catalyst with Li-doped alumina as support was more readily desulfated than the undoped analog, a fact attributed to the formation of smaller Ba sulfate crystals [14]. Recently, Corbos and co-workers [15, 16] studied the effect of support oxide and Ba loading on the sulfur resistance and desulfation of model Pt/BaO/support LNT catalysts. BaO supported on Al–Si and Ce–Zr mixed oxides was found to exhibit higher NO_x storage capacity after exposure to sulfating conditions in comparison with BaO supported on alumina. Moreover, the use of ceria-zirconia as support was found to result in a decrease in bulk $BaSO_4$ stability under H_2 relative to alumina.

In this paper, we report on another strategy to improve the sulfur resistance of LNT catalysts, based on the addition of ceria to the main $Pt/BaO/Al_2O_3$ phase. Ceria is well known as an important component of LNTs formulated for lean burn gasoline applications, its role being to provide the necessary oxygen storage capacity under stoichiometric operation, i.e., when the LNT is required to function as a conventional three-way catalyst. Previously we have observed that incorporation of ceria in LNTs not only improves NO_x storage efficiency but also positively impacts LNT regeneration behavior [17, 18]. Rohart et al. [19, 20] have also studied the effect of adding rare earth oxides, including CeO_2 and $Ce–ZrO_2$, to $Pt/BaO/Al_2O_3$ catalysts. Among other effects, they found that the presence of these ceria-containing oxides lowered the temperature required for catalyst desulfation. In addition, Theis and co-workers have reported that the addition of ceria can improve NO_x trap sulfur tolerance [21]. Studies on three-way catalysts have shown that ceria is able to store sulfur (as sulfate) [22], while the use of ceria for trapping SO_2 and NO_x in commercial FCC regenerating units is well known [23]. Consequently, it can be reasoned that the presence of ceria in a LNT catalyst may help to protect the main NO_x storage component from sulfur poisoning. To ascertain whether this is correct, we have studied the effect of ceria addition on the sulfation/desulfation behavior of model powder LNT catalysts.

2 Experimental

2.1 Catalyst Preparation

Pt/CeO_2 and $Pt/BaO/Al_2O_3$ powders were prepared by incipient wetness impregnation. CeO_2 (Rhodia, surface area of 119 m^2/g) was impregnated with an aqueous solution of tetraammineplatinum(II) nitrate, then dried and calcined in air at 500 °C for 3 h. $Pt/BaO/Al_2O_3$ was prepared in a sequential manner. Alumina (Sasol, γ-phase, surface area of 132 m^2/g) was first impregnated with aqueous $Ba(OOCCH_3)_2$, then dried and calcined at 500 °C in air. The Ba-loaded Al_2O_3 was subsequently impregnated with aqueous tetraammineplatinum(II) nitrate and further calcined at 500 °C. The Pt loading of both materials was 1 wt.%, and the BaO content of the $Pt/BaO/Al_2O_3$ sample was 20 wt.%. To prepare a ceria-containing catalyst, a portion of $Pt/BaO/Al_2O_3$ was physically mixed with Pt/CeO_2 in a 74:26 weight ratio. This ratio was chosen based on typical Ba:Ce ratios used in gasoline lean burn LNT catalysts.

2.2 NO_x Storage Capacity (NSC) and Temperature Programmed Desulfation

A microreactor loaded with ca. 150 mg of powder catalyst was employed to study the NO_x storage properties of the catalysts in the pretreated, sulfated and desulfated states. In all cases the feed gas flow rate corresponded to a gas hourly space velocity (GHSV) of 30,000 h^{-1}. Effluent gases were analyzed using a mass spectrometer (SRS RGA100). The pretreatment consisted of exposing the catalyst to flowing 1% H_2/Ar at 750 °C for 1 h, followed by cooling to 300 °C in the flowing gas. To measure the NO_x storage capacity of the catalyst, the sample was exposed to lean conditions consisting of 300 ppm NO, 10% O_2, 5% CO_2 and 5% H_2O in Ar (120 sccm total flow rate). This was followed by a 15 min exposure to rich conditions (1% H_2, 5% CO_2 and 5% H_2O in Ar at 120 sccm), after which a second 60 min lean/15 min rich cycle was performed. The NO_x storage capacity was subsequently calculated from the NO_x uptake during a third 60 min lean phase.

Catalyst sulfation was accomplished at 300 °C under cycling conditions consisting of one 60 min lean/15 min rich cycle, followed by one 60 min lean phase; 27 ppm SO_2 was included in the feed for each of these conditions. The SO_2 flow was then shut off and the catalyst exposed to a second 15 min rich phase. The NO_x storage capacity of the catalyst was measured during the subsequent (third) 60 min lean phase. After the NO_x storage measurement, the sulfur poisoned catalysts were desulfated according to the temperature programmed method, using the rich phase gas mixture (including 5% CO_2 and H_2O). The temperature was ramped at a rate of 10 °C/min from 300 to 700 °C and held at this temperature for 1 h. After cooling to 300 °C, the NO_x storage capacity was re-measured using the same conditions used for the pretreated catalyst.

2.3 DRIFTS Study

In order to understand the role of ceria in mitigating sulfur poisoning of the Ba phase, DRIFTS was applied to monitor the sulfur species involved in catalyst sulfation and desulfation. DRIFTS measurements were performed in an integrated stainless-steel reaction cell, using a MIDAC model M2500 FTIR spectrometer coupled with a Harrick Scientific barrel ellipsoidal mirror DRIFT accessory. The system is typically operated at slightly below atmospheric pressure (around 500 Torr) to prevent stagnation in the cell and to maintain the seal between the removable hemispherical ZnSe dome and the cell body. Tylan General mass flow controllers were used to establish the inlet gas concentrations, in conjunction with a sparger system submerged in a NESLAB RTE-110 recirculating constant temperature bath that controlled the inlet concentration of H_2O. Additional details of this system are described elsewhere [24, 25].

Catalysts were first pretreated overnight to minimize the presence of $BaCO_3$ using cycling conditions (15 min lean: 300 ppm NO and 10% O_2 in Ar; 10 min rich: 1% H_2/Ar) at 350 °C. After the pretreatment, the catalysts were heated to 550 °C and background DRIFT spectra were recorded every 50 °C while cooling to 300 °C. The catalyst was then exposed to lean gas containing 27 ppm SO_2 at 300 °C, DRIFT spectra being recorded continuously for the duration of the sulfation (30 min). The DRIFTS cell was then flushed with Ar and cooled to 200 °C prior to desulfation. Next, the gas flow was switched from Ar to 1% H_2/Ar and the sample was heated at a ramp rate of 10 °C/min to 550 °C. During this process DRIFT spectra were recorded every 50 °C. The sample was held at 550 °C under flowing 1% H_2/Ar for 30 min, after which the temperature was lowered in 50 °C steps so that additional DRIFT spectra could be acquired. To measure the adsorbed species on the catalyst after these steps, the DRIFT spectra must be compared to the original background spectra. Our results are reported in terms of absorbance units which are calculated using the formula:

$$\text{Absorbance} = -\log_{10}\left[\frac{\text{Sample file}}{\text{Background file}}\right]$$

For comparison to realistic exhaust conditions, the effect of H_2O addition on the sulfation behavior of the LNT catalysts was also investigated in this study. This was done by adding 5% H_2O to the lean gas mixture used during the catalyst sulfation measurements.

3 Results and Discussion

3.1 Effect of Sulfation on NO_x Storage Capacity

Two model catalysts were used in this work, namely Pt/BaO/Al_2O_3 (hereafter denoted as PBA), and a physical mixture of Pt/BaO/Al_2O_3 and Pt/CeO_2 (74:26 weight ratio, denoted as PBAC). To quantify the effect of ceria incorporation on catalyst sulfation and desulfation behavior, NO_x storage measurements were performed for pretreated, sulfated and desulfated samples of both PBA and PBAC. Figure 1 presents the outlet NO_x concentration profiles during the measurements. For PBA, large differences in NO_x storage capacity (NSC) were found between the

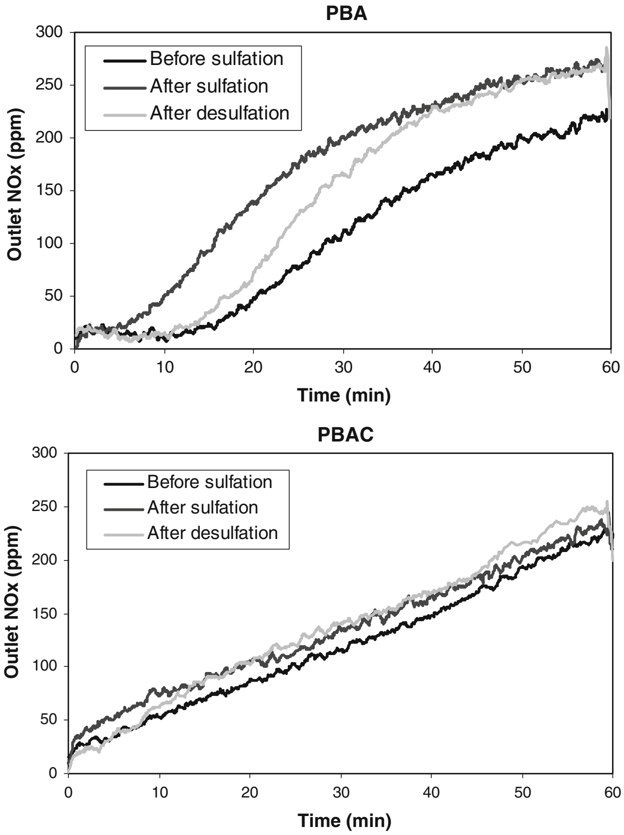

Fig. 1 Outlet NO_x concentration as a function of time during NO_x storage under lean conditions; top: PBA, bottom: PBAC. Gas composition: 300 ppm NO, 10% O_2, 5% CO_2, 5% H_2O, Ar balance, GHSV = 30,000 h^{-1}

Table 1 Comparison of NO_x storage capacity and H_2S released during temperature-programmed desulfation

Catalyst	NO*x* stored[a] (μ mol/g_{cat})			SO2 fed (μ mol/g_{cat})			H2S released[b] (μ mol/g_{cat})		
	Before sulfation	After sulfation	After desulfation	Lean	Rich	Total	CeO2	BaO	Total
PBA	400	271	322	111	14	125	–	87	87
PBAC	373	343	339	110	14	124	19	55	74

[a] Lean phase for NO_x storage: 300 ppm NO, 10% O_2, 5% CO_2, 5% H_2O, Ar balance, GHSV = 30,000 h^{-1}

[b] Rich phase for TPR: 1% H_2, 5% CO_2, 5% H_2O, Ar balance, GHSV = 30,000 h^{-1}

samples. Sulfation caused a pronounced decrease in both the short term (~10 min) and long term (60 min) NSC. The accumulated NO_x stored for a period of 60 min dropped from 400 μmol/g_{cat} for the pretreated sample to 271 μmol/g_{cat} after sulfation (see Table 1), corresponding to a 32% decline in NSC. From Fig. 1, it is apparent that subsequent desulfation improved the storage capacity but was unable to restore the long term NSC to its original value. Although NO_x storage increased from 271 μmol/g_{cat} for the sulfated sample to 322 μmol/g_{cat} after desulfation, this represents a 20% drop in NSC compared to the value measured prior to sulfation. This suggests that the applied desulfation temperature of 700 °C is insufficient to remove all of the stored sulfur; indeed, several literature reports indicate that a temperature in excess of 700 °C is required for the decomposition of "bulk" $BaSO_4$, corresponding to either large $BaSO_4$ crystallites and/or Ba sulfate located far away from Pt sites [26, 27]. Additionally, it is possible to convert the sulfates to sulfides under rich conditions at high temperatures, specifically on the Ba phase [26, 28, 29]. Although desulfating in the presence of H_2O minimizes sulfide formation [30, 31], sulfide can still form in measurable quantities, resulting in less sulfur evolved. During desulfation, sulfur was released almost exclusively as H_2S, with a negligible amount of SO_2 being evolved (see Sect. 3.2 below). Table 1 shows that the amount of H_2S released from each catalyst was less than the total amount of SO_2 fed to the reactor. Formation of sulfides would explain this observation, and can account for the residual loss in NSC following desulfation. Thermal aging at 700 °C is expected to have a minimal impact on catalyst NSC, especially since the pretreatment was performed at 750 °C.

Relative to PBA, PBAC showed rather different trends in NO_x uptake behavior after sulfation and desulfation. Sulfation caused a decrease in short term NSC, while the long term storage capacity was little changed. As seen in Table 1, NSC dropped from 373 μmol/g_{cat} at 60 min prior to sulfation to 343 μmol/g_{cat} for the sulfated catalyst, corresponding to an ~8% decrease. According to Fig. 1, desulfation restored the short term storage capacity, although the long term NSC was not improved. Indeed, the NSC measured at 60 min was marginally worse after desulfation. Although this result was unexpected, a possible explanation can be found in the results presented here.Sulfur is observed to release from the ceria phase at around 450 °C, as shown below, mainly as H_2S. At this temperature, its re-adsorption is likely on the less sulfated Ba phase, resulting in a stable Ba sulfide. Consequently, this sulfur was not completely removed during the desulfation process. Overall, however, the presence of ceria is still beneficial, the decrease in NSC after one sulfation–desulfation cycle being 9% for PBAC, as compared 20% for PBA.

3.2 Temperature-Programmed Desulfation

In order to provide more insight into their desulfation behavior, temperature-programmed reduction (TPR) experiments were performed on sulfated samples of PBA and PBAC. During H_2-TPR sulfur was released from both catalysts mainly as H_2S; the resulting H_2S and SO_2 release profiles are shown in Fig. 2. For PBA, release of H_2S occurred at ~650 °C, whereas PBAC showed two discrete H_2S release events at ~450 °C and ~650 °C. From this it follows that the H_2S release at ~450 °C corresponds to desulfation of the ceria phase, a finding confirmed by the results of DRIFTS measurements performed during the desulfation of a Pt/CeO_2 reference sample (see section 3.3.2), while Ba desulfation occurs at the higher temperature. Additionally, we cannot exclude the possibility that a small portion of the sulfur released at high temperature may originate from the alumina support [26].

The amount of H_2S released from the catalysts during desulfation is shown in Table 1. While PBA exhibited a total H_2S release of 87 μmol/g_{cat}, that from PBAC was slightly lower at 74 μmol H_2S/g_{cat}; of this, 19 μmol H_2S/g_{cat} originated from the CeO_2 phase and 55 μmol H_2S/g_{cat} from the Ba phase. Significantly, the ratio between the amount of H_2S released from the Ba phase in PBAC and PBA is 0.63, being lower than the weight ratio of the Ba phase in PBAC (0.74). This implies that the addition of ceria decreased the degree of sulfation of the main Ba NO_x storage component.

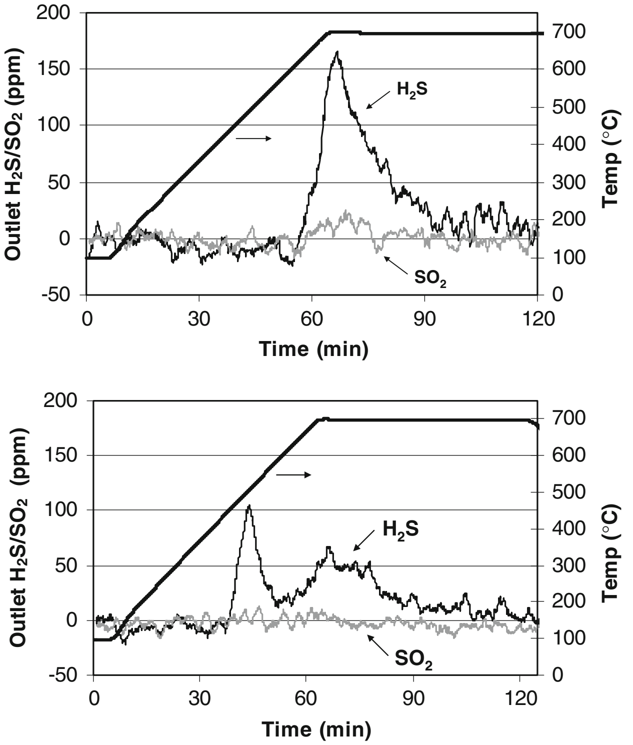

Fig. 2 Sulfur release during temperature-programmed desulfation (1% H_2, 5% H_2O and 5% CO_2 in Ar); top: sulfated PBA, bottom: sulfated PBAC

3.3 DRIFTS Measurements

3.3.1 PBA

To better understand the effect of ceria on LNT sulfation and desulfation behavior, a DRIFTS study was performed using samples of PBA and PBAC. The catalysts were exposed to sulfating conditions at 300 °C (lean conditions with 27 ppm SO_2 added), in both the absence and presence of added H_2O; in each case, DRIFT spectra were recorded as a function of time, as shown in Fig. 3, the main spectral features being summarized in Table 2. In the absence of H_2O, the spectra of PBA at short exposure times featured bands at 1,418, 1,323 and 1,039 cm^{-1}, corresponding to Ba nitrate species [4, 32]. With increased exposure time, a new broad band appeared at 1,130 cm^{-1} which became progressively stronger; this can be attributed to Ba sulfate [4, 33, 34]. After 30 min of exposure, nitrate bands were still observable.

When H_2O was added to the feed gas, significant changes in SO_x and NO_x adsorption behavior were observed. As shown in Fig. 3b, Ba sulfate bands started to appear in the region 1,250–1,000 cm^{-1} at a much earlier stage than in the absence of H_2O, i.e., after ~2 min of exposure. An additional band at 978 cm^{-1} can be ascribed to Al sulfite [34]. In addition, the presence of Al sulfate cannot be excluded, given that the expected bands at 1,350 and 1,040 cm^{-1} would overlap with the nitrate bands at 1,320 and 1,039 cm^{-1}. The intensity of the nitrate bands attained a maximum at 10 min of exposure, after which their intensity gradually decreased. In contrast, the sulfate bands became progressively more intense, indicating that nitrate species were displaced by sulfate. After 30 min of adsorption, sulfate species dominated the spectrum.

3.3.2 PBAC

PBAC exhibited similar IR spectra to PBA when H_2O was absent (see Fig. 3c), with the exception of two additional bands at 1,542 and 1,516 cm^{-1}. These bands can be ascribed to nitrate species formed on ceria, as reported in our previous study [35]. As shown in Fig. 3d, when H_2O was added to the $SO_2/NO/O_2$ feed, the bands formed at 1,542 and 1,516 cm^{-1} were very weak, consistent with previous observations that competitive adsorption by H_2O partially suppresses the formation of nitrates on CeO_2 [35]. The dominant bands in the spectra again corresponded to Ba nitrates and Ba sulfate. Significantly, both sets of bands continued to grow in intensity during the course of the experiment, suggesting that nitrate and sulfate were able to form at different sites on the catalyst.

In order to better compare the sulfation behavior of PBA with that of PBAC, the DRIFT spectra recorded after 30 min of sulfation are collected in Fig. 4. In the absence of H_2O, the ratio of sulfate/nitrate band intensities was similar for both PBA and PBAC (~0.4). However, when the feed contained H_2O, the sulfate/nitrate ratio for PBA increased from 0.4 to 2.4, whereas the ratio for PBAC was only slightly increased (0.4–0.5). Clearly, while the addition of H_2O increased the degree of sulfation of both catalysts, the presence of ceria resulted in the retention of significant NO_x storage capacity. The promoting effect of H_2O addition on sulfation has been reported previously. Using IR spectroscopy, Abdulhamid et al. [34] observed increased formation of bulk Ba sulfate in a Ba-based LNT catalyst when H_2O was added to the SO_2/O_2 feed. In this study, it was difficult to distinguish the relative amounts of bulk and surface sulfate formed since the main sulfate band was very broad. The presence of nitrate bands in the spectra also hindered the observation of bulk Ba sulfate. A possible explanation for the promoting effect of H_2O on sulfation involves its role in improving the adsorption and transport of SO_x on the catalyst surface. The presence of H_2O should favor the formation of surface hydroxyl groups on the alumina support, which can act as SO_2 adsorption sites with the formation of HSO_3^- species [36, 37]. Ba sulfation would then result from the migration of these species and their reaction with the more basic Ba phase.

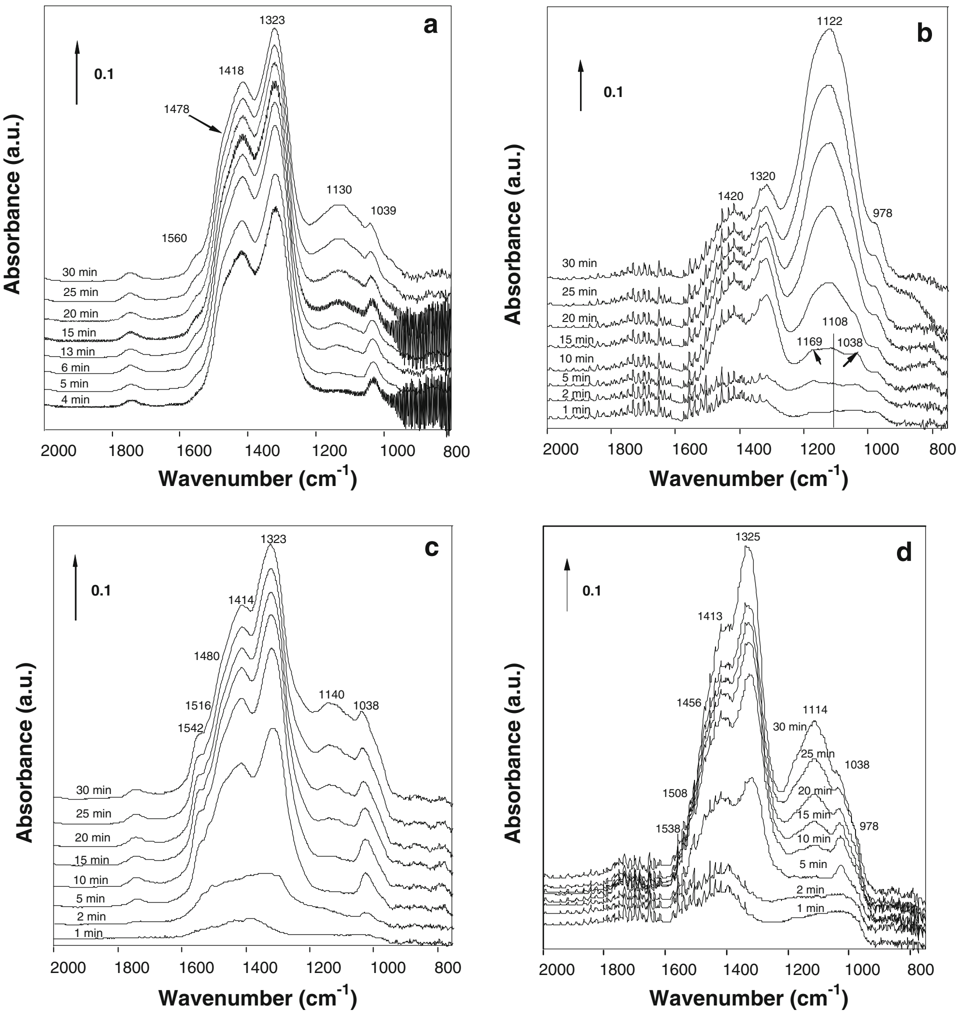

Fig. 3 DRIFT spectra obtained upon exposure of PBA and PBAC to $SO_2/NO/O_2$: **a** PBA, with dry feed; **b** PBA, with 5% H_2O added to feed; **c** PBAC, with dry feed; **d** PBAC, with 5% H_2O added to feed

Table 2 Summary of observed DRIFT spectral features

Phase	Surface/bulk species	Wavenumber (cm^{-1})	Reference
Barium	Nitrate	1,414–1,420	[4, 32]
		1,320–1,323	
		1,038–1,039	
	Sulfate	1,120–1,130	[4, 33, 34]
Alumina	Nitrate	1,560	[40–42]
	Sulfate	1,350, 1,040	[33, 34, 43]
	Sulfite	970–980	[34]
Ceria	Nitrate	1,540, 1,516	[35]
	Sulfite/sulfate	1,193, 1,085, 978, 880	[38, 39]

In order to better understand the behavior of ceria during sulfation, an additional sulfation experiment was performed using Pt/CeO_2 in flowing $SO_2/NO/O_2$ at 300 °C. As shown in Fig. 5 (top), cerium sulfite and sulfate bands [38, 39] appeared in the range 1,400–800 cm^{-1} at an early stage of the exposure (around $\sim$2 min). Nitrate and sulfate (or sulfite) bands grew in simultaneously during the first 10 min of adsorption, after which the nitrate bands became weaker and the sulfate bands became stronger with time. After 30 min of exposure, the spectrum was dominated by the sulfate bands, indicating that almost all of the nitrate species were replaced by sulfate. These results confirm the idea that ceria can function as an efficient storage medium for SO_x; as shown in Fig. 3d, in a Ba-based LNT catalyst, this can mitigate the effects of sulfur poisoning by lessening the amount of sulfur stored on the Ba NO_x storage component.

Finally, the stability of sulfated Pt/CeO_2 was examined under rich conditions. DRIFT spectra were acquired as a function of temperature under an atmosphere of flowing 1% H_2/Ar. As shown in Fig. 5 (bottom), the intensity of the sulfate bands was significantly decreased at 400 °C, removal of the sulfate being complete at 450 °C. This finding is in accordance with the temperature-programmed desulfation results presented in Fig. 2. It should be noted that since the DRIFT spectra were acquired in the absence of H_2O, it is likely that the sulfates were reduced to sulfides [26], rather than being converted to H_2S or SO_2. However,

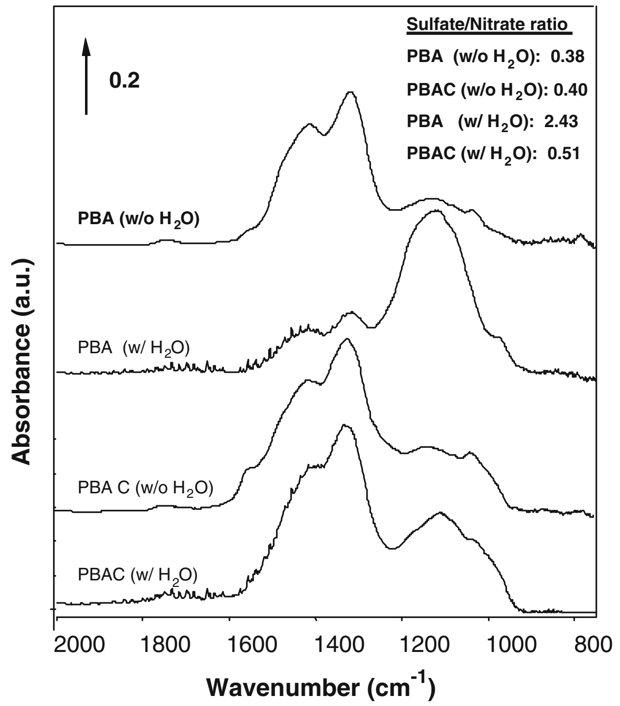

Fig. 4 Comparison of DRIFT spectra after 30 min of sulfation at 300 °C for PBA and PBAC

control experiments (not shown) indicate that the temperature at which sulfate is converted to sulfide/H_2S is not noticeably influenced by the presence of water.

4 Conclusions

The results from this study show that the addition of ceria to Ba-based LNT catalysts exerts a positive effect on LNT performance in the presence of sulfur. After sulfation, higher NO_x storage capacity was measured for the model ceria-containing catalyst used in this work than its non-ceria analog, suggesting that ceria is able to store sulfur and thereby mitigate sulfation of the main (Ba) NO_x storage phase. DRIFTS measurements performed under a flowing feed of $NO/O_2/SO_2/H_2O$ support this view, as do the results of TPR experiments. In the latter, desulfation of the ceria-containing catalyst was found to occur in two stages, corresponding to sulfur elimination from the ceria phase at ~450 °C, followed by sulfur loss from the Ba phase at ~650 °C. Significantly, the ceria-containing catalyst displayed relatively lower sulfur evolution from the Ba phase than its non-ceria analog, confirming that the presence of ceria lessened the degree of sulfur accumulation on the Ba phase.

A practical benefit of these findings is that it may be possible to extend the operating period between desulfation events for ceria-containing LNTs; this would have the advantage of reducing the associated fuel penalty, and, more importantly, slowing the decline in catalyst performance with time due to thermal aging phenomena such as the sintering of precious metal particles.

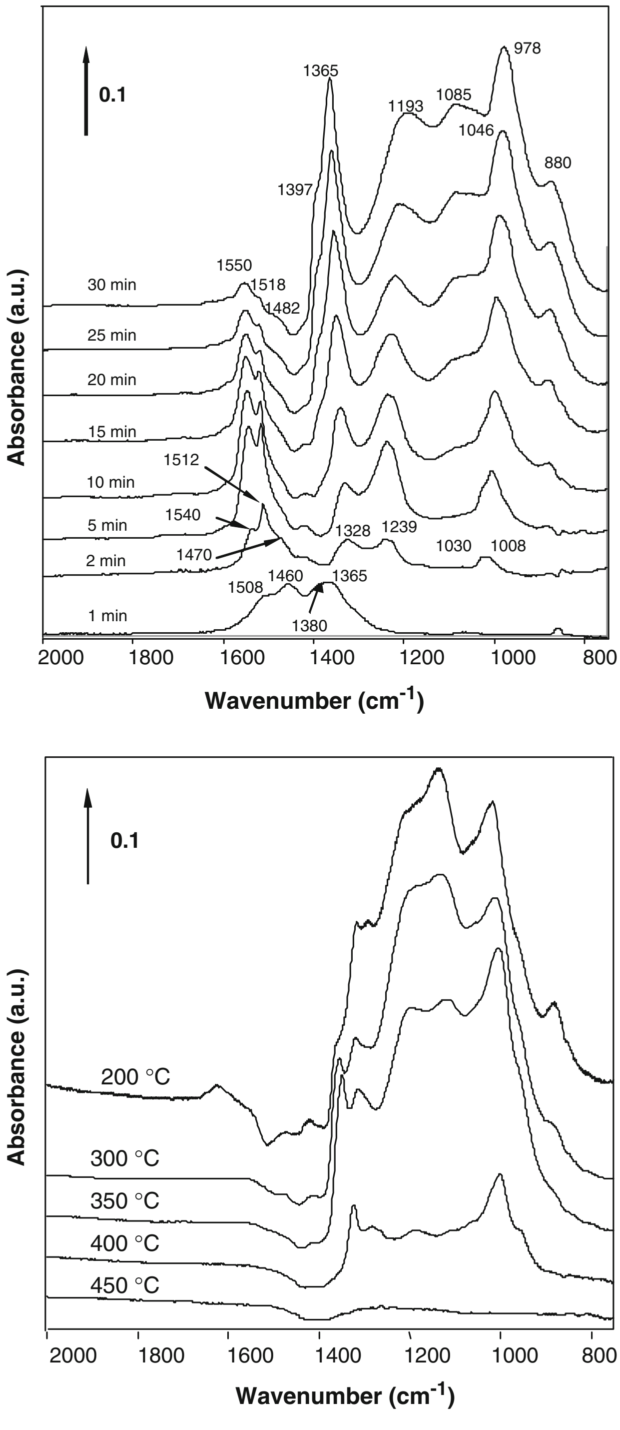

Fig. 5 DRIFT spectra of Pt/CeO2; top: during sulfation in flowing SO2/NO/O2 at 300 °C, bottom: during desulfation in flowing 1% H2/Ar

Acknowledgments This publication was prepared with the support of the U.S. Department of Energy, under Award No. DE-FC26-05NT42631. However, any opinions, findings, conclusions, or recommendations expressed herein are those of the authors and do not necessarily reflect the views of the DOE.

References

1. Epling WS, Campbell LE, Yezerets A, Currier NW, Parks JEII (2004) Cat Rev Sci Eng 46(2):163
2. Narula CK, Daw CS, Hoard JW, Hammer T (2005) Int J Appl Ceram Technol 2:452
3. Yamazaki K, Suzuki T, Takahashi N, Yokota K, Sugiura M (2001) Appl Catal B 30:459
4. Fanson PT, Horton MR, Deglass WN, Lauterbach J (2003) Appl Catal B 46:393
5. Basile F, Fornasari G, Grimandi A, Livi M, Vaccari A (2006) Appl Catal B 69:58
6. Huang HY, Long RQ, Yang RT (2001) Appl Catal B 33:127
7. Hodjati S, Petit C, Pitchon V, Kiennemann A (2001) Appl Catal B 30:247
8. Hepburn JS, Watkins WLH (1998) US Patent 5,758,489
9. Yamamoto K, Kikuchi R, Takeguchi T, Eguchi K (2006) J Catal 238:449
10. Centi G, Fornasari G, Gobbi C, Livi M, Trifiro F, Vaccari A (2002) Catal Today 73:287
11. Clacens JM, Montiel R, Kochkar H, Figueras F, Guyon M, Beziat JC (2004) Appl Catal B 53:21
12. Matsumoto S, Ikeda Y, Suzuki H, Ogai M, Miyoshi N (2000) Appl Catal B 25:115
13. Hachisuka I, Hirata H, Ikeda Y, Matsumoto S (2000) SAE Technical Paper 2000-01-1196
14. Miyoshi N, Matsumoto S (1999) Stud Surf Sci Catal 121:245
15. Corbos EC, Courtois X, Bion N, Marecot P, Duprez D (2008) Appl Catal B 80:62
16. Corbos EC, Elbouazzaoui S, Courtois X, Bion N, Marecot P, Duprez D (2007) Top Catal 42–43:9
17. Ji Y, Toops TJ, Crocker M (2007) Catal Lett 119:257
18. Ji Y, Choi J-S, Toops TJ, Crocker M, Naseri M (2008) Catal Today 136:146
19. Rohart E, Belleière-Baca V, Yokota K, Harlé V, Pitois C (2007) Top Catal 42–43:71
20. Belleière-Baca V, Harlé V, Pitois C, Rohart E, Allain M (2007) SAE Technical Paper 2007-01-1241
21. Theis J, Ura J, Goralski C Jr, Jen H, Thanasiu E, Graves Y, Takami A, Yamada H, Miyoshi S (2003) SAE Technical Paper 2003-01-1160
22. Truex T (1999) SAE Technical Paper 1999-01-1543
23. Trovarelli A, de Leitenburg C, Boaro M, Dolcetti G (1999) Catal Today 50:353
24. Powell GL, Milosevic M, Lucania J, Harrick NJ (1992) Appl Spec 46:111
25. Toops TJ, Smith DB, Partridge WP (2005) Appl Catal B 58:245
26. Elbouazzaoui S, Corbos EC, Courtois X, Marecot P, Duprez D (2005) Appl Catal B 61:236
27. Yu Stakheev A, Gabrielsson P, Gekas I, Teleguina NS, Bragina GO, Tolkachev NN, Baeva GN (2007) Top Catal 42–43:143
28. Limousy L, Mahzoul H, Brilhac JF, Garin F, Maire G, Gilot P (2003) Appl Catal B 45:169
29. Kim DH, Szanyi J, Kwak JH, Szailer T, Hanson J, Wang CM, Peden CHF (2006) J Phys Chem B 110:10441
30. Toops TJ, Pihl JP (2006) Presented at the 9th CLEERS (Crosscut lean exhaust emissions research simulations) Workshop, Dearborn, MI, May
31. Kim DH, Kwak JH, Wang XQ, Szanyi J, Peden CHF (2008) Catal Today 136:183
32. Desikusumastuti A, Staudt T, Gronbeck H, Libuda J (2008) J Catal 255:127
33. Sedlmair Ch, Seshan K, Jentys A, Lercher JA (2002) Catal Today 75:413
34. Abdulhamid H, Fridell E, Dawody J, Skoglundh M (2006) J Catal 241:200
35. Ji Y, Toops TJ, Graham UM, Jacobs G, Crocker M (2006) Catal Lett 110:29
36. Lavalley JC, Janin A, Preud'homme J (1981) React Kinet Catal Lett 18:85
37. Davydov A, Sheppard N (2003) Molecular spectroscopy of oxide catalyst surfaces. Wiley, Chichester, pp 146–157
38. Waqif M, Bazin P, Saur O, Lavalley JC, Blanchard G, Touret O (1997) Appl Catal B 11:193
39. Bazin P, Saur O, Lavalley JC, Blanchard G, Visciglio V, Touret O (1997) Appl Catal B 13:265
40. Abdulhamid H, Dawody J, Fridell E, Skoglundh M (2006) J Catal 244:169
41. Anderson JA, Liu Z, Garcia MF (2006) Catal Today 113:25
42. Toops TJ, Smith DB, Epling WS, Parks JE, Partridge WP (2005) Appl Catal B 58:255
43. Datta A, Cavell RG, Tower RW, George ZM (1985) J Phys Chem 89:443